

# Rapid Quantitation of High-Speed Flow Jets

Krishna S. Nayak,<sup>1\*</sup> Bob S. Hu,<sup>1,2</sup> and Dwight G. Nishimura<sup>1</sup>

**Flow jets containing velocities up to 5–7 m/s are common in patients with congenital defects and patients with valvular disease (stenosis and regurgitation). The quantitation of peak velocity and flow volume in these jets is clinically significant but requires specialized imaging sequences. Conventional 2DFT phase contrast sequences require lengthy acquisitions on the order of several minutes. Conventional spiral phase contrast sequences are faster, but are highly corrupted by flow artifacts at these high velocities due to phase dispersion and motion during the excitation and readout. A new prospectively gated method based on spiral phase contrast is presented, which has a sufficiently short measurement interval (<4 ms) to minimize flow artifacts, while achieving high spatial resolution ( $2 \times 2 \times 4 \text{ mm}^3$ ) to minimize partial volume effects, all within a single breathhold. A complete single-slice phase contrast movie loop with 22 ms true temporal resolution is acquired in one 10-heartbeat breathhold. Simulations indicate that this technique is capable of imaging through-plane jets with velocities up to 10 m/s, and initial studies in aortic stenosis patients show accurate in vivo measurement of peak velocities up to 4.2 m/s (using echocardiography as a reference). Magn Reson Med 50:366–372, 2003. © 2003 Wiley-Liss, Inc.**

**Key words:** MR flow quantitation; phase contrast; spirals; aortic stenosis

Flow jets containing velocities up to 5–7 m/s are common in patients with congenital defects and patients with valvular disease (stenosis and regurgitation). In these patients, the quantification of peak velocity and flow volume is clinically significant but requires specialized MR imaging sequences. Several groups have reported accurate in vivo measurement of high velocities (1–5). However, long 2DFT-based phase contrast acquisitions required both respiratory and cardiac motion compensation (gating plus navigators) resulting in scan times on the order of 2–4 min per CINE movie loop and 30–60 min per study.

Significantly faster velocity-mapping sequences were developed by incorporating spiral and echo-planar readout trajectories (6–9). These sequences could achieve high spatial resolution within the confines of a single breathhold, but suffer from local image artifacts near high speed and/or complex flows. With subsequent hardware improvements, real-time and interactive color flow mapping

systems were also developed (10), based on spiral phase contrast.

These spiral and EPI-based phase contrast techniques, while time-efficient, are highly susceptible to flow artifacts in the presence of fast and turbulent flow. This is due to a combination of effects: 1) phase dispersion within voxels, 2) through-plane motion during the excitation, and 3) in-plane motion during readouts. The most severe of these artifacts are signal voids due to insufficient spatial resolution (allowing phase dispersion within voxels), and blurring and ghosting artifacts due to in-plane motion during long spiral or EPI readouts. These artifacts can be minimized by designing for higher spatial resolution and shortening readout length, respectively.

In this article, we present a prospectively gated breathheld method based on spiral phase contrast (6,7) which has a sufficiently short measurement interval (<4 ms, from the start of the RF to the end of the readout) and readout time (2.2 ms) to minimize flow artifacts, while achieving high in-plane resolution ( $2 \times 2 \text{ mm}^2$ ) to minimize partial volume effects, all within a single breathhold. A complete single-slice phase contrast movie loop with 22 ms true temporal resolution can be acquired in one 10-heartbeat breathhold. Bloch simulations indicate that this technique is capable of imaging and quantifying through-plane flow jets with velocities up to 10 m/s. Initial studies on healthy volunteers and aortic stenosis patients show accurate in vivo measurement of peak velocity in jets up to 4.2 m/s, using echocardiography as a reference. Image quality is compared against a real-time color flow sequence (10), also based on spiral phase contrast, which was used for localization in the in vivo studies.

## MATERIALS AND METHODS

The imaging pulse sequence (Fig. 1) consisted of a slice-selective excitation, bipolar gradient, short spiral readout, and gradient spoiler, achieving a TR of 5.5 ms and TE of 1.6 ms. We used a slice thickness of 4 mm, imaging flip angle of  $20^\circ$ , and velocity encoding (VENC) between 1.47 and 6.05 m/s, depending on the subject. The VENC was chosen to be roughly 20–50% above the expected peak velocity to avoid aliasing while providing maximum sensitivity.

The primary design goals were achieving high spatial resolution and minimizing the readout duration (to mitigate in-plane flow artifacts). Using optimal spiral trajectory design based on our scanner configuration (11–13), we were able to achieve 2.0 mm resolution over a 20 cm FOV using 2.2 ms spiral readouts with 20 interleaves. This was achieved without any undersampling. A rapid  $480 \mu\text{s}$  slice selective excitation was used to minimize the echo time and minimize through-plane flow artifacts. This type of excitation also excites lipid signal, which is thought to be acceptable in this application because of the physical dis-

<sup>1</sup>Magnetic Resonance Systems Research Laboratory, Department of Electrical Engineering, Stanford University, Stanford, California.

<sup>2</sup>Division of Cardiovascular Medicine, Palo Alto Medical Foundation, Palo Alto, California.

Grant sponsors: National Institutes of Health; GE Medical Systems.

Preliminary accounts of this work were presented at the 10th annual meeting of the ISMRM, Honolulu, 2002 (abstract #1720) and the 6th annual scientific sessions of the Society for Cardiovascular Magnetic Resonance, Orlando, February, 2003 (abstract #138).

\*Correspondence to: Krishna S. Nayak, Packard Electrical Engineering, Room 216, 350 Serra Mall, Stanford University, Stanford, CA 94305-9510. E-mail: nayak@mrsrl.stanford.edu

Received 29 October 2002; revised 11 April 2003; accepted 11 April 2003.

DOI 10.1002/mrm.10538

Published online in Wiley InterScience (www.interscience.wiley.com).

© 2003 Wiley-Liss, Inc.

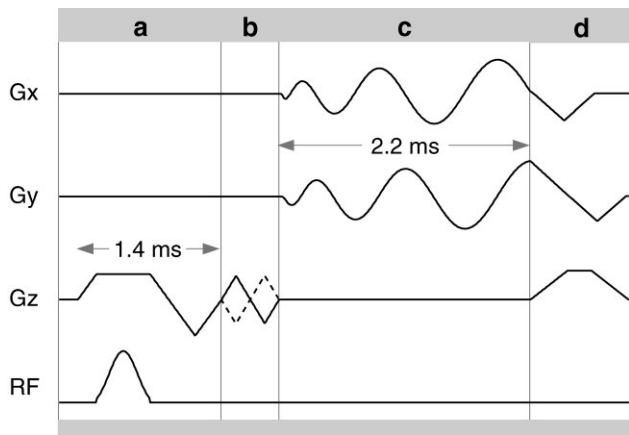


FIG. 1. Pulse sequence consists of (a) 480  $\mu$ s RF slice selective excitation, (b) 640–960  $\mu$ s flow-encoding gradient, (c) 2.2 ms spiral readouts, and (d) refocusing and spoiler gradients.

tance between fat and the flow of interest. An added benefit of such short spiral readouts is the reduction of spiral off-resonance blurring. In this sequence, typical  $B_0$  inhomogeneity will result in insignificant blurring and lipid signal will only be blurred by about 2 mm.

Bloch simulations were performed using Matlab (MathWorks, South Natick, MA) for a variety of through-plane and in-plane flow velocities. Simulations of linear constant-velocity flow were used to establish flow properties of the sequence. Through-plane flow sensitivity of the excitation was analyzed by producing effective slice profiles for various through-plane velocities and flip angles (14). In-plane flow sensitivity of the readout was analyzed by producing velocity point spread functions for various in-plane velocities (15,16).

10-heartbeat breath hold, 22 ms per image

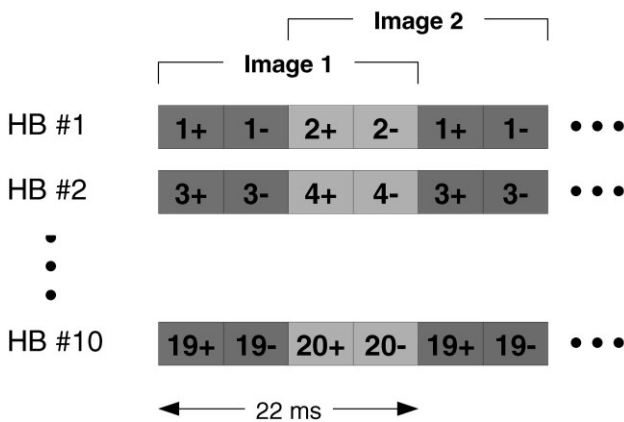


FIG. 2. Acquisition timing during a 10-heartbeat breathhold. Each box represents one measurement and one imaging TR (5.5 ms). Inside are the interleaf number and the sign of the flow encoding gradient. 20-interleaves with positive and negative flow encoding are used to form each image. The true temporal resolution is 22 ms and a sliding window reconstruction is used to produce a new image every 11 ms.

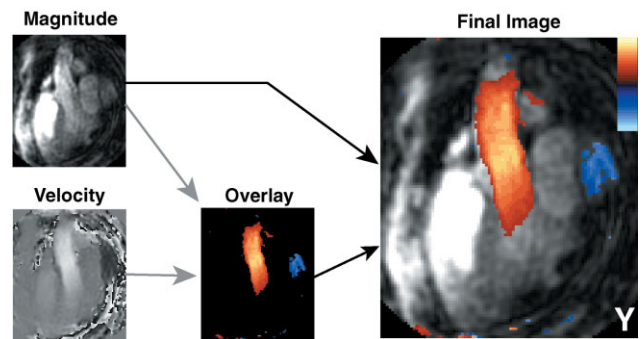


FIG. 3. Color overlay. CINE phase contrast videos were displayed using a color overlay similar to ultrasound. Images are acquired with two different flow encodings. A magnitude image is computed from the magnitude sum of the two images, and a velocity image is computed from the phase difference. A color overlay is created using an ultrasound colormap (clipped to highlight high velocities in locations where there is sufficient signal). The final image is the overlay plane superimposed onto the magnitude image.

In vivo studies were performed on a GE Signa 1.5 T CV/i scanner (General Electric, Waukesha, WI), equipped with gradients capable of 40 mT/m magnitude and 150 T/m/sec slew rate and a receiver capable of 4  $\mu$ sec sampling ( $\pm 125$  kHz). A body coil was used for RF transmission and a 5-inch surface coil was used for signal reception. The institutional review board of Stanford University approved the imaging protocols. Each subject was screened for MRI risk factors and provided informed consent in

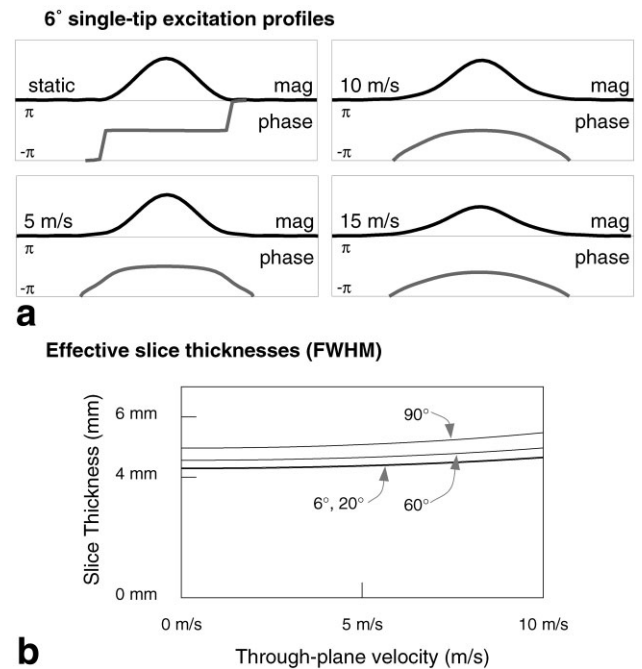


FIG. 4. Bloch simulations of through-plane flow during excitation. Simulated (a) excitation profiles for through-plane flow up to 10 m/s demonstrate reasonable slice profiles and flat phase. The (b) effective slice thicknesses calculated as the full-width at half-max (FWHM) of the excitation profile is within 30% of design for flow up to 10 m/s.

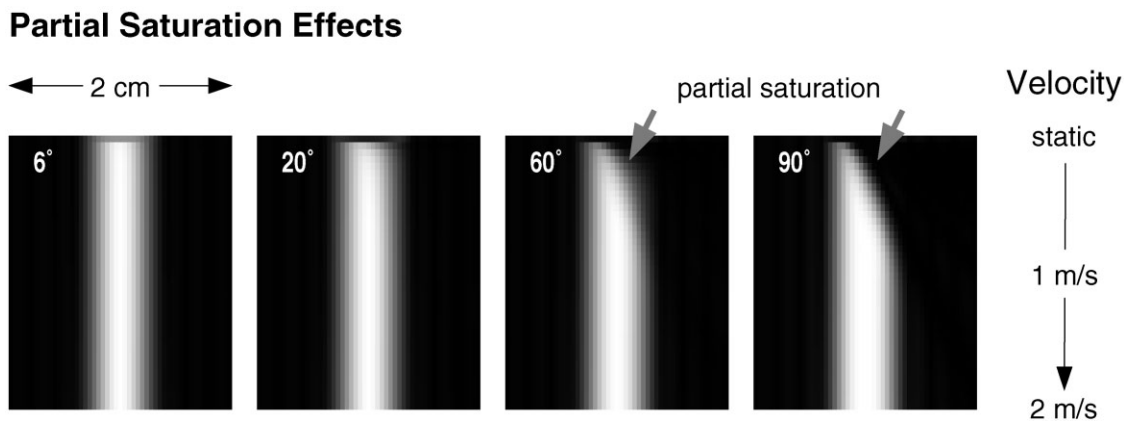


FIG. 5. Bloch simulations of the partial saturation effects particularly affecting high flip angles and low velocities. In each image, labeled by an imaging flip angle, the vertical axis represents through-plane velocity. Each horizontal line in each image contains a magnitude slice profile for that particular flip angle and through-plane velocity (black = low signal, white = high signal). Partial saturation of spins moving slower than 1 m/s warps the effective slice profile (shown by gray arrows) for flip angles around 60–90°.

accordance with institutional policy. The patient protocol involved first localizing scan planes using an existing real-time interactive color flow system (10). This system was not optimized for fast flow and used a 30 ms TR, 5 ms TE, 7 ms spectral-spatial excitation, and 12.4 ms spiral readout trajectories. Real-time video clips of 5–10 sec were recorded at each relevant cardiac view and appropriate slice prescriptions were then rescanned using the proposed gated sequence during 10-heartbeat breathholds. Each breathheld scan produced a CINE color-flow movie with 40–70 cardiac phases using a sliding window reconstruction. Acquisitions were prospectively ECG-triggered. The timing of acquisitions is illustrated in Fig. 2.

Color flow movies were generated from each dataset. Each temporal frame was formed by first reconstructing complete images for the positive and negative flow encodes. A magnitude image was taken as the sum of the two images, while a velocity image was computed as the phase difference between the two images. A color overlay, previously described (10), was then used to overlay the velocity information over the anatomical magnitude image. The image display path is illustrated in Fig. 3. Frames were assembled to form a color-flow movie from each dataset. Over operator-defined regions of interest (ROIs) covering the flow of interest, velocity-time histograms were produced. Peak velocity measurements were made based on these histograms.

## RESULTS AND DISCUSSION

### Simulations

#### Through-Plane Flow

Bloch simulations of through plane flow were performed to establish sensitivity of the sequence to signal loss due to motion during the excitation. Figure 4a contains the effective slice profiles for a variety of through-plane velocities with a flip angle of 6°. Through-plane velocities up to 10 m/s provide a reasonably flat-phased signal, while beyond about 15 m/s the phase profile of the excitation varies noticeably across the slice, causing some signal loss. In

addition, the effective slice width increases with increasing flow velocity. Figure 4b illustrates the increase in effective slice thickness as a function of velocity for a few different flip angles. Slice thickness is measured as the full-width at half-maximum (FWHM) of the excitation profile. For through-plane velocities up to 10 m/s, the effective slice thickness increase is less than 30%.

Another factor to consider when using gradient-spoiled sequences (especially those with short TR) is potential

### Velocity Point Spread Functions

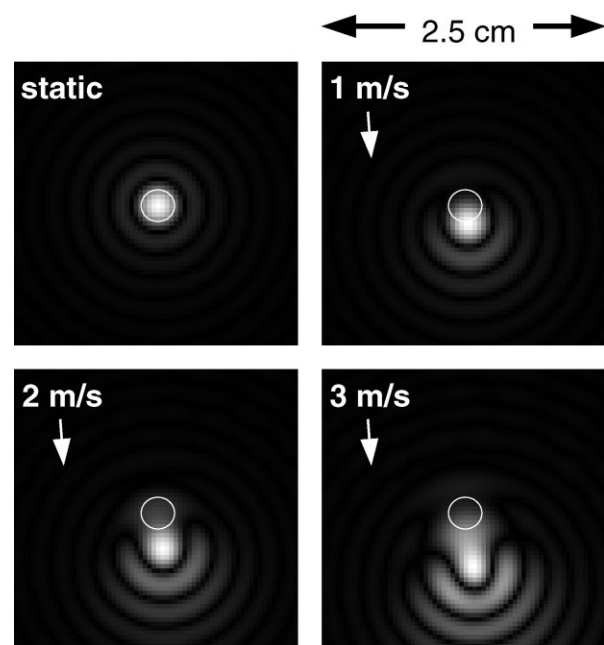


FIG. 6. Bloch simulations of in-plane flow during readout and acquisition. Image artifacts due to in-plane flow can be characterized by a velocity point spread function (PSF). Simulations of in-plane velocities up to 2 m/s exhibit reasonable PSF blurring and distortion in the direction of flow and a displacement by 0–2 mm. Beyond an in-plane velocity of 2 m/s, artifacts are more severe.

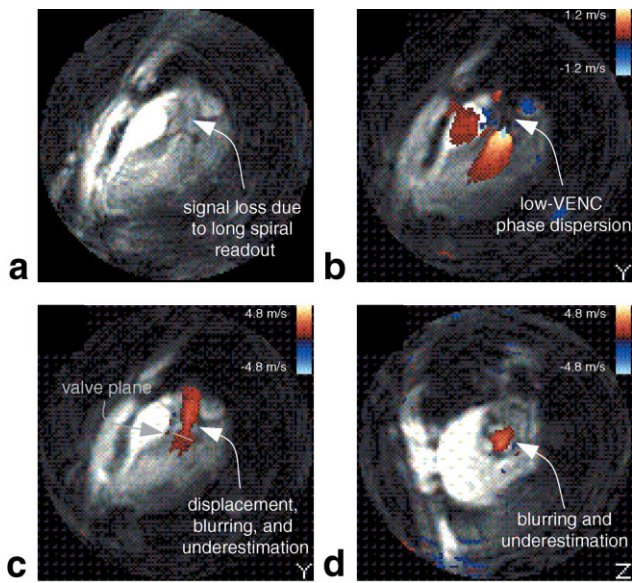


FIG. 7. Conventional real-time (21) and real-time color flow (10) sequences experience a multitude of artifacts in and around fast flow jets, limiting quantitative analysis. The images shown are from a patient with a 4.2 m/s AS jet as measured by echocardiography, and illustrate (a) flow voids due to motion during 12.4 ms long spiral readouts, (b) signal loss due to phase dispersion when using a low VENC, and (c,d) underestimation of the true peak velocity by roughly 30% even when using an appropriate VENC due to partial voluming. Displacement artifacts due to the 4 ms echo time are clearly seen in c. The lack of highly spatially resolved flow information is seen in all images.

artifact due to partial saturation of spins moving slowly in the slice-select direction. At a TR of 5.5 ms or shorter, such effects can occur even for spins moving at 1 m/s. For flip angles from 1–90°, and velocities from 0–15 m/s, Bloch simulations were performed to find the effective steady

state slice profile. Shown in Fig. 5 are images of effective slice profiles (horizontal axis) for velocities between 0 and 2 m/s (vertical axis), at a few different flip angles. It is clear that when using flip angles well above 20°, partial saturation effects become significant even for spins moving as fast as 50–75 cm/s. In our in vivo studies, we used a flip angle of 20° to avoid this effect. However, higher flip angles may be used since the pathologic velocities of interest ( $\geq 2$  m/s) are unaffected even at high flip angles.

*In-Plane Flow*

Short spiral acquisitions produce reasonably small displacement and blurring artifacts for in-plane flow up to about 2 m/s. Figure 6 contains velocity point-spread functions (PSF) for static and a few different in-plane velocities. At less than 2 m/s the shift is less than one resolution element, in this case 2 mm. In addition, there is some low-amplitude PSF distortion in the direction of the flow. When in-plane velocity exceeds about 2.5 m/s the PSF distortion is more severe, and causes blurring in the direction of flow, which can lead to displacement artifact, loss of spatial resolution, and partial volume effects when signals from multiple spatial locations fall into the same reconstructed voxel (17).

Note that the target application for this sequence is the quantification of through-plane jets containing velocities up to 7 m/s; therefore, resilience to a reduced range of in-plane velocities ( $< 2$  m/s) is acceptable. If targeting higher in-plane velocities, the spiral readouts could be further shortened by reducing each spiral’s curvature and/or extent. This would either require more interleaves or result in lower image resolution. Projection reconstruction (PR) readouts would enable the widest range of in-plane velocity measurement but would drastically reduce scan efficiency.

**Healthy Subject aortic outflow**

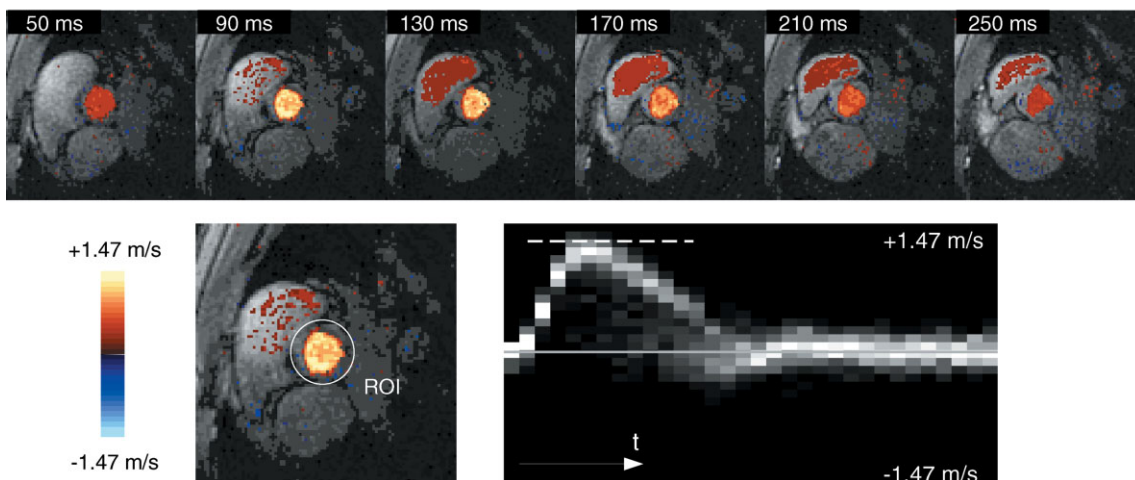
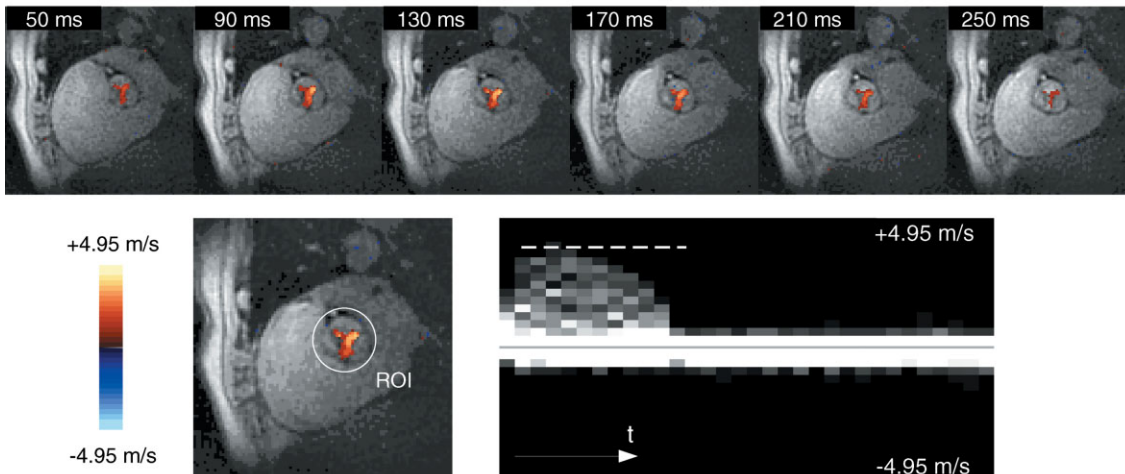


FIG. 8. Short-TR spiral phase contrast in a healthy volunteer: CINE color flow loops and time-velocity waveforms were acquired in single breathholds. Selected frames from a movie taken at the aortic valve plane are shown. Peak velocity was measured to be  $\approx 1.4$  m/s. A “plug flow”-like profile is observed in both the video and time-velocity histogram.

### Patient 1 aortic stenosis



### Patient 2 aortic stenosis

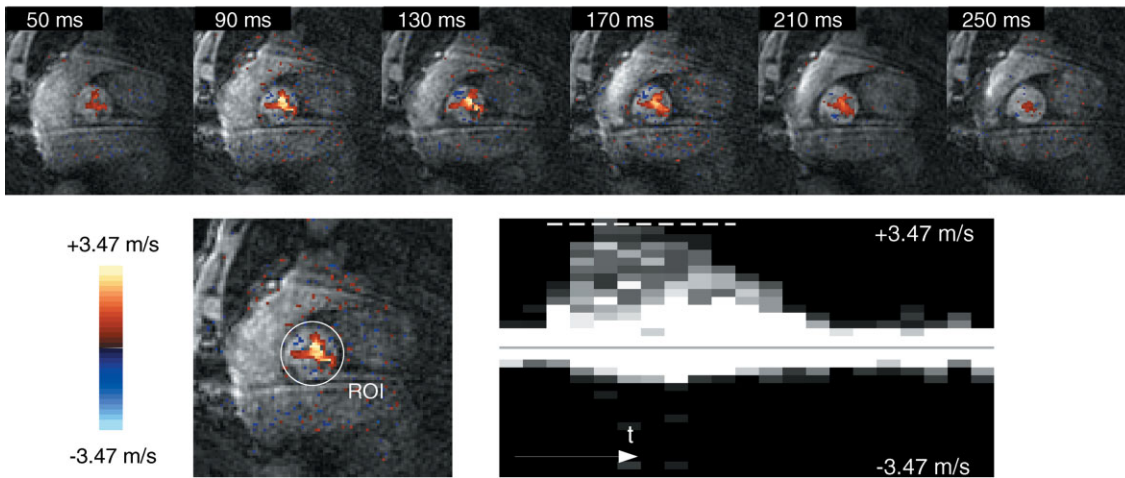


FIG. 9. Short-TR spiral phase contrast in two AS Patients: CINE color flow loops and time-velocity waveforms acquired in single breathholds. In these two patients (#1 is the same as in Fig. 7), 45 cardiac phases were acquired in each 10-sec breathhold. Selected frames from cross-sectional views of the aortic root are shown, using through-plane flow encoding. Adjacent to each are time-resolved velocity histograms, which were generated by plotting measured velocities within a region of interest (ROI) around the aorta in each slice. Peak velocities were within 20% of echocardiography measurements.

#### Off-Resonance

In spiral imaging, off-resonance causes an additional blurring when more than  $\pi/4$  of phase accrues during a readout (18). At 1.5 T,  $B_0$  homogeneity around the heart is typically within 70 Hz (19,20), and our experience indicates that the aortic root can be easily shimmed to within 20 Hz. For 2.2-ms readouts, off-resonance blurring for this range is insignificant.

Lipid signal at 1.5 T ( $-220$  Hz from water) experiences about  $\pi/2$  of phase during our readouts and experience slight blurring (roughly one pixel). This should not hinder visualization of cardiac fat and blood flow in our studies due to the distance between fat and flowing blood. In addition, because we used echo times of 1.5–2 ms, lipid and water are almost completely out of phase, causing noticeable signal reduction in areas of fat.

#### In Vivo Studies

In an initial set of in vivo studies, four healthy subjects and four patients with aortic stenosis (AS) were recruited. In each volunteer, scan planes containing cross sections of the aortic root were localized and scanned with real-time color flow (10), and then with the proposed sequence. Velocity encoding was set to encode 1.47 m/s (960  $\mu$ s bipolar) in healthy subjects and 3.47 m/s to 6.05 m/s (720  $\mu$ s to 640  $\mu$ s bipolar) in AS patients. The VENC was chosen to be roughly 20–50% above the expected peak velocity to avoid aliasing while providing maximum sensitivity.

Figure 7 contains images from the localization portion of one patient study and illustrates many of the artifacts common in real-time and real-time color flow imaging. These include signal loss during long spiral readouts

Table 1  
Measured Peak Velocities in Four Aortic Stenosis Patients

Patient	Echo	MRI
#1	4.20 m/s	4.0 m/s
#2	4.20 m/s	3.47 m/s
#3	4.05 m/s	3.9 m/s
#4	2.67 m/s	2.51 m/s

(15,16), signal loss due to phase dispersion when using a low VENC, displacement artifacts due to the long echo time, blurring due to motion during spiral readouts, and subsequent partial volume effects resulting in peak velocity underestimation.

In normal volunteers scan plane localization using the real-time color flow system took roughly 4 min. Five breathheld scans were then performed at a prescribed slice containing the aortic valve plane. Figure 8 contains images from one of the healthy volunteer studies, in which a peak velocity of 1.4 m/s was measured and normal aortic valve function was clearly visualized. Total scan time was less than 20 min for all volunteers.

Figure 9 contains images from two patient studies. Patient 1 had a moderate aortic stenosis, with a mean gradient of 42 mmHg, aortic valve area (AVA) of 0.87 cm<sup>2</sup>, and peak velocity of 4.2 m/s evaluated by echocardiography. Patient 2 also had moderate aortic stenosis, with a mean gradient of 38 mmHg, AVA of 1.0 cm<sup>2</sup>, and peak velocity of 4.2 m/s evaluated by echocardiography. Frames are shown spanning the first 300 ms of systole. Notice that coherent signal from these high-speed flow jets were achieved in both studies. Peak velocities (see Table 1) and velocity-time waveforms were comparable to echocardiography in all four patient studies. Note that in Patient 2 peak velocity was underestimated, most likely due to angle effects (the slice not being perpendicular to the flow jet).

As magnitude and velocity information are available at each frame, it also became possible to visualize leaflets in cross section. Figure 10 contains a few frames from Patient 1. The limited tricuspid valve opening is visualized even in the magnitude image, potentially enabling direct valve area measurement.

Finally, in addition to stenosis, this sequence may be applicable to the imaging of regurgitant flow jets and flow jets in patients with congenital heart disease. Figure 11 contains sample images from a patient with aortic regurgitation and a patient with an atrial septal defect. In both cases flow jets were clearly visualized, without any nearby signal loss.

**CONCLUSIONS**

We have presented a short-TR spiral phase contrast sequence that is capable of imaging and measuring high-speed flow jets during short breathholds. Simulations indicate that the accurate measurement of through-plane flows up to 10 m/s is possible. Preliminary in vivo results have shown agreement with echocardiography in a cohort of patients with jet velocities up to 4.2 m/s. A larger clinical trial is under way at our institution. Such a sequence may also be useful for quantifying volume flow

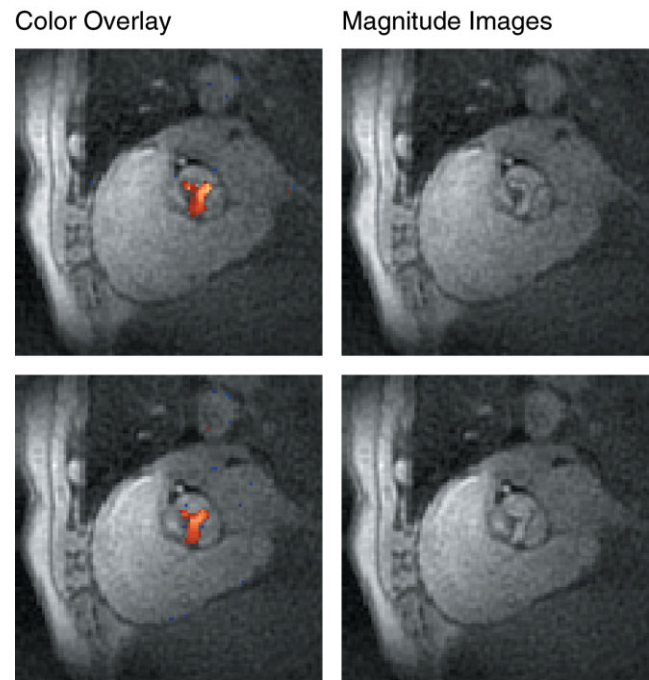


FIG. 10. Color overlay and magnitude-only images from Patient 1. As flow artifacts are minimized, it is also possible to visualize and potentially measure valve area directly from magnitude images.

and, in particular, regurgitant volume. For that application, compensation for partial saturation (shown in Fig. 5) will be necessary.

One important concern when measuring peak velocity is the angle  $\alpha$  between the flow jet and the flow-encoding direction. The measured velocities will underestimate true velocities by a factor of  $\cos(\alpha)$ . For small angles this effect is also small; however, in the case of eccentric jets, angle effects may cause significant underestimation. This can be remedied by 1) rapidly scanning with multiple directions of flow encoding to resolve full velocity vectors, or 2) using a localization sequence that is capable of better visualizing such jets, to ensure that the slice prescriptions are indeed perpendicular to the predominant flow.

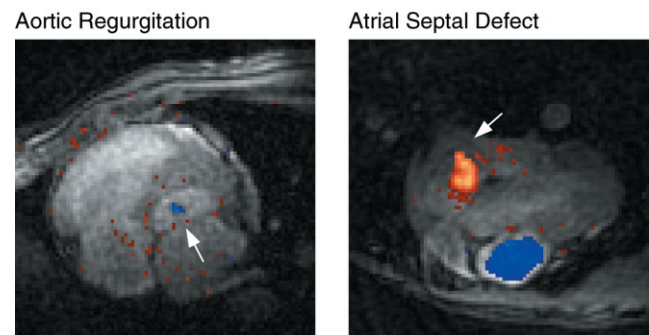


FIG. 11. Short-TR spiral phase contrast in a patient with valvular regurgitation and a patient with a congenital defect. Individual frames from (left) a cross-sectional view of the left ventricular outflow tract showing an aortic regurgitation, and (right) an oblique view illustrating flow through an atrial septal defect.

Our current implementation of this sequence, achieves  $2 \times 2 \text{ mm}^2$  in-plane resolution, 4 mm slice thickness, and is capable of measuring high-speed jets in a single breath-hold. The acquisition time for each image is 220 ms, which, if segmented over 10 heartbeats, results in 22 ms temporal resolution, and if segmented over five heartbeats, results in 44 ms temporal resolution. A speed-up of 15–20% is immediately possible with pulse sequence optimizations such as incorporating the flow encoding into the slice-select gradient and reducing the dead time between the spoiler and end of TR. With these improvements, and sacrificing some spatial resolution for increased temporal resolution, a true real-time version of this sequence may be possible.

## ACKNOWLEDGMENTS

The authors thank Brian Hargreaves for allowing us to adapt his pulse sequence and Julie DiCarlo for useful discussions. We also thank Patricia Nguyen, Miriam Amitai, and Michael McConnell for help in recruiting and performing the patient studies.

## REFERENCES

- Kilner PJ, Firmin DN, Rees RSO, Martinez J, Pennell DJ, Mohiaddin RH, Underwood SR, Longmore DB. Valve and great vessel stenosis: assessment with MR jet velocity mapping. *Radiology* 1991;178:229–235.
- Kilner PJ, Manzara CC, Mohiaddin RH, Pennell DJ, Sutton MG, Firmin DN, Underwood SR, Longmore DB. Magnetic resonance jet velocity mapping in mitral and aortic valve stenosis. *Circulation* 1993;87:1239–1248.
- Eichenberger AC, Jenni R, von Schulthess GK. Aortic valve pressure gradients in patients with aortic valve stenosis: quantification with velocity-encoded cine MR imaging. *Am J Roentgenol* 1993;160:971–977.
- Sondergaard L, Hildebrandt P, Lindvig K, Thomsen C, Stahlberg F, Kassis E, Henriksen O. Valve area and cardiac output in aortic stenosis: quantification by magnetic resonance velocity mapping. *Am Heart J* 1993;126:1156–1164.
- Sondergaard L, Stahlberg F, Thomsen C, Stensgaard A, Lindvig K, Henriksen O. Accuracy and precision of MR velocity mapping in measurement of stent cross-sectional area, flow rate, and pressure gradient. *J Magn Reson Imag* 1993;3:433–437.
- Pike GB, Meyer CH, Brosnan TJ, Pelc NJ. Magnetic resonance velocity imaging using a fast spiral phase contrast sequence. *Magn Reson Med* 1994;32:476–483.
- Gatehouse PD, Firmin DN, Collins S, Longmore DB. Real time blood flow imaging by spiral scan phase velocity mapping. *Magn Reson Med* 1994;31:504–512.
- McKinnon GC, Debatin JF, Wetter DR, Schulthess GK. Interleaved echo planar flow quantification. *Magn Reson Med* 1994;32:263–267.
- Debatin JF, Leung DA, Wildermuth S, Botnar R, Felblinger J, McKinnon GC. Flow quantitation with echo-planar phase-contrast velocity mapping: in vitro and in vivo evaluation. *J Magn Reson Imag* 1995;5:656–662.
- Nayak KS, Pauly JM, Kerr AB, Hu BS, Nishimura DG. Real-time color flow MRI. *Magn Reson Med* 2000;43:251–258.
- Meyer CH, Pauly JM, Macovski A. A rapid, graphical method for optimal spiral gradient design. In: *Proc 4th Annual Meeting ISMRM*, New York, 1996. p 392.
- Meyer CH, Pauly JM. A rapid method of optimal gradient waveform design for k-space scanning in MRI. US Patent Number 6,020,739, 2000.
- King KF, Foo TKF, Crawford CR. Optimized gradient waveforms for spiral scanning. *Magn Reson Med* 1995;34:156–160.
- Fredrickson JO, Meyer CH, Pelc NJ. Flow effects of spectral spatial excitation. In: *Proc 5th Annual Meeting ISMRM*, Vancouver, 1997. p 113.
- Nishimura DG, Irarrazabal P, Meyer CH. A velocity k-space analysis of flow effects in echo-planar and spiral imaging. *Magn Reson Med* 1995;33:549–556.
- Gatehouse PD, Firmin DN. Flow distortion and signal loss in spiral imaging. *Magn Reson Med* 1999;41:1023–1031.
- Nishimura DG, Jackson JL, Pauly JM. On the nature and reduction of the displacement artifact in flow images. *Magn Reson Med* 1991;22:481–492.
- Noll DC, Meyer CH, Pauly JM, Nishimura DG, Macovski A. A homogeneity correction method for magnetic resonance imaging with time-varying gradients. *IEEE Trans Med Imag* 1991;10:629–637.
- Reeder SB, Faranesh AZ, Boxerman JL, McVeigh ER. In vivo measurement of  $T_2^*$  and field inhomogeneity maps in the human heart at 1.5 T. *Magn Reson Med* 1998;39:988–998.
- Jaffer FA, Wen H, Balaban RS, Wolff SD. A method to improve the  $B_0$  homogeneity of the heart in vivo. *Magn Reson Med* 1996;36:375–383.
- Kerr AB, Pauly JM, Hu BS, Li KCP, Hardy CJ, Meyer CH, Macovski A, Nishimura DG. Real-time interactive MRI on a conventional scanner. *Magn Reson Med* 1997;38:355–367.